

RoFL: Attestable Robustness for Secure Federated Learning

Lukas Burkhalter*, Hidde Lycklama à Nijeholt*, Alexander Viand, Nicolas Küchler, Anwar Hithnawi

ETH Zürich

Abstract

Federated Learning is an emerging decentralized machine learning paradigm that allows a large number of clients to train a joint model without the need to share their *private data*. Participants instead only share ephemeral updates necessary to train the model. To ensure the confidentiality of the client updates, Federated Learning systems employ secure aggregation; clients encrypt their gradient updates, and only the aggregated model is revealed to the server. Achieving this level of data protection, however, presents new challenges to the robustness of Federated Learning, i.e., the ability to tolerate failures and attacks. Unfortunately, in this setting, a malicious client can now easily exert influence on the model behavior without being detected. As Federated Learning is being deployed in practice in a range of sensitive applications, its robustness is growing in importance. In this paper, we take a step towards understanding and improving the robustness of secure Federated Learning. We start this paper with a systematic study that evaluates and analyzes existing attack vectors and discusses potential defenses and assesses their effectiveness. We then present RoFL, a secure Federated Learning system that improves robustness against malicious clients through input checks on the encrypted model updates. RoFL extends Federated Learning’s secure aggregation protocol to allow expressing a variety of properties and constraints on model updates using zero-knowledge proofs. To enable RoFL to scale to typical Federated Learning settings, we introduce several ML and cryptographic optimizations specific to Federated Learning. We implement and evaluate a prototype of RoFL and show that realistic ML models can be trained in a reasonable time while improving robustness.

1 Introduction

Machine learning algorithms continue to achieve remarkable success in a wide range of applications. These advancements are possible, in part, due to the availability of large domain-specific datasets for training machine learning models. Hence, there are expanding efforts to collect more data to train models

for new applications. However, this data collection poses severe privacy issues, hampering efforts to bring machine learning benefits to sensitive sectors, e.g., health. This, in turn, has led to a surge [2, 4, 37, 71] in interest in privacy-preserving solutions for machine learning. Federated Learning and Collaborative Learning have recently emerged as alternative machine learning paradigms that eliminate the need to pool data centrally. The privacy risks associated with the large-scale collection of sensitive data and the rise of privacy regulations that give users control over their data make these learning paradigms a compelling alternative for sensitive applications.

Federated Learning (FL) [54] is a decentralized learning paradigm that allows a service to train and improve a machine learning model without the need to have direct access to the training data. The training process is distributed across a set of participants who collaborate to train a joint global model through an iterative process of aggregating locally trained updates. In contrast to the conventional (logically) centralized machine learning [48], data remains local at the sources in FL. Its main benefit lies in its ability to retain data locally (i.e., data ownership and sovereignty) and it is enticing for scenarios where data privacy and liability are a concern [31, 54]. Today, FL is used to train models for a variety of privacy-sensitive applications [15, 16, 62, 63, 66, 67].

Decoupling training from the need to pool data centrally does not by itself guarantee data privacy or security in FL; client updates may still reveal sensitive information about the underlying training data [14, 56]. Therefore, *secure* FL systems employ *secure aggregation* [14, 31, 81] to prevent the client updates from leaking information to the server during aggregation. Clients send encrypted updates to the server, which can recover only the aggregated joint model update. The participants’ ability to run a copy of the model *locally* in FL and keep their data, and the training process opaque from the server brings many privacy benefits. However, in this setting, malicious clients can directly replace and influence the joint model behavior in a way that is not possible in the centralized learning paradigm. Hence, this exposes FL to a range of powerful new vulnerabilities that currently presents a core challenge to the *robustness* of FL.

*These authors contributed equally to this work.

Federated Learning Robustness. The decentralized and distributed nature of FL makes it inherently vulnerable to arbitrary failures [12, 80] and targeted attacks (i.e., model update poisoning) [5, 7]. Shortly after the introduction of FL a flurry of work has exposed the severity of these attacks [5, 7, 78]. Arbitrary failures and un-targeted attacks can easily prevent or slow learning [12, 80]. While undesirable, this predominately impacts convergence and will eventually be detected as the server can observe that the model accuracy is not improving. Targeted attacks¹, on the other hand, present a core issue to the robustness of FL, as they pose a severe threat to model integrity. Hence, in this work, we primarily focus on this class of attacks.

Defenses against malicious clients frequently build on the assumption that benign and malicious client’s updates are distinguishable [12, 36, 80]. Hence they augment aggregation protocols with audits to detect these malicious updates [12, 36, 68, 80]. Initial results show that these defenses might not necessarily maintain their effectiveness in the FL setting [5, 78]. Moreover, these solutions cannot easily be applied to *secure* FL systems, which, by design, do not allow audits of individual updates (i.e., data confidentiality). In order to realize practical robustness guarantees for secure FL, we need to understand the causes of these attacks and use this understanding to design mitigation strategies that are efficient and secure in preventing them.

This paper brings two contributions towards understanding and improving the robustness of Secure FL:

① **Understanding the Robustness of FL:** Even after seeing a large number of attacks exposing severe vulnerabilities in FL, we still lack a holistic understanding of what enables these attacks and how they can be effectively mitigated. In order to improve our understanding of FL robustness, we demystify the inner workings of existing attacks. We answer, via an empirical analysis, why these attacks are possible and why a definitive solution to FL robustness is challenging. We then analyze and discuss solutions that can improve FL robustness. We show that for some severe attacks, constraints on client updates can effectively improve robustness. We make our framework for analyzing FL robustness available online². We hope our analysis can help practitioners deploying FL better assess the implications and risks of using an *open* learning process.

② **RoFL.** In this work we present RoFL, a secure FL system design that enables expressing and enforcing constraints on high-dimensional encrypted model updates. At its core, RoFL augments existing secure FL aggregation protocols with zero-knowledge proofs that allow the server to enforce and verify constraints on client updates. Specifically, we integrate L_∞ / L_2 -norm bound checks within RoFL. Realizing these checks using zero-knowledge proofs [44], presents a

paramount challenge to the *scalability* of FL. To enable practical cryptographic proofs on high dimensional vectors, RoFL uses comparatively efficient zero-knowledge constructions that incur a low bandwidth overhead [17] for the required constraints. However, these improvements alone are not sufficient to permit RoFL to scale to realistic ML models. Therefore, we introduce several optimizations at the ML layer that allow us to reduce the number of necessary cryptographic checks while preserving the effectiveness of our defenses. With our targeted optimizations, our protocol can scale to realistic model sizes as seen in FL deployments. These optimizations allow for 5x and 6-7x reduction of required cryptographic checks for the L_2 and L_∞ respectively. Our end-to-end evaluation of RoFL shows that RoFL can realize secure FL for a CIFAR-10 model with 273k parameters, requiring only about 6x the computation time as a non-secure baseline that provides neither robustness nor confidentiality. We make RoFL’s prototype available online³.

2 Evaluating and Understanding the Robustness of Federated Learning

Though there has been a flurry of works that exposed FL’s vulnerability to attacks [5, 7, 74, 78, 79], we currently lack a comprehensive and systematic understanding of FL robustness. This analysis aims to fill in this knowledge gap by demystifying the inner working of existing attacks and providing technical insights about FL robustness in practice.

Federated Learning Background. FL is a form of collaborative learning that allows a server to train a machine learning model using data that is scattered across a large number of decentralized clients. In this learning paradigm, an FL server coordinates the training of a machine learning model $f_{\mathbf{w}_G}$ parametrized by weights $\mathbf{w}_G \in \mathbb{R}^d$ where d is the number of parameters, based on data held locally by a set of clients N with size $n = |N|$. The server instantiates a learning process that aims at minimizing an empirical loss $\sum_{(x,y) \in D} \ell(y, f_{\mathbf{w}_G}(x))$ where ℓ is the loss function and D is the union of the n client datasets D_1, \dots, D_n . At each round of the iterative learning process, the server (i.e., aggregator) selects a subset of m clients N_m from the set of available clients N . After the client selection process, the server broadcasts the current global model \mathbf{w}_G^t at round t to the selected clients. Afterwards, each client $i \in [1, m]$ locally runs a training algorithm \mathcal{A} starting from the current global model \mathbf{w}_G^t to create their next local model \mathbf{w}_i^{t+1} using local training data D_i with the goal of minimizing the local empirical loss, i.e., $\sum_{(x,y) \in D_i} \ell(y, f_{\mathbf{w}_i^t}(x))$. Each client then sends its local update $\Delta \mathbf{w}_i^{t+1} := \mathbf{w}_i^{t+1} - \mathbf{w}_G^t$ back to the aggregation server. The server aggregates the updates into a new global model \mathbf{w}_G^{t+1} , i.e., $\mathbf{w}_G^{t+1} = \mathbf{w}_G^t + \frac{\eta}{n} \sum_{i=1}^m \Delta \mathbf{w}_i^{t+1}$, where η is the global learning rate. This process repeats until the server terminates the training process.

¹In targeted attacks, the attacker aims to make the global model misbehave on specific inputs (i.e., integrate a backdoor into the model).

²<https://github.com/pps-lab/fl-analysis>

³<https://github.com/pps-lab/rofl-project-code>

Federated learning is inherently open to a multitude of participants – often in the orders of thousands – and, as a consequence, the training algorithm in this setting can be susceptible to contributions from compromised clients. Throughout this analysis we assume the adversary can compromise up to a fraction $\alpha \in [0, 1]$ of clients in N_m . A compromised client i can submit a malicious update $\Delta\hat{\mathbf{w}}_i^{t+1}$ to the aggregation server, with the goal to perturb the benign global model \mathbf{w}_G to a poisoned version $\hat{\mathbf{w}}$.

What makes FL robustness challenging? Besides being susceptible to the known security and privacy vulnerabilities encountered in the typical machine learning setting, FL exposes new attack surfaces. Moreover, several FL characteristics elevate the impact of attacks known in the centralized setting (e.g., backdoor attacks through data poisoning) [5, 7, 78]. More specifically, these unique challenges are attributed to: (i) *Open Nature*: In FL the training process is open and often involves a large number of participants where any participant can act maliciously. (ii) *Attackers Capabilities*: In conventional centralized learning settings, an adversary can instigate targeted attacks only by data poisoning. In the FL setting, however, an adversary can do so by directly manipulating model updates to enhance its impact (e.g., scaling), allowing more effective attacks. (iii) *Active Attackers*: An attacker that controls a subset of clients can observe and influence the model behavior over multiple training rounds, which can allow for a stronger form of adaptive attacks.

In this analysis, we focus on attacks where the adversary aims to influence the final trained model’s behavior such that it behaves maliciously on a specific sub-task while maintaining good accuracy on the main task. We find that adversaries broadly exploit two different vulnerabilities (i.e., aggregation and memorization) in the FL pipeline to achieve this adversarial goal. As these vulnerabilities are structurally different, we study them in isolation and then conclude with a discussion on how to improve FL robustness in light of these vulnerabilities.

2.1 Attack Strategies

Adversarial Goals. We consider an attacker that aims to integrate a backdoor into the global model [5, 7, 74], i.e., cause it to misclassify a subset of *unmodified* data samples, while maintaining high accuracy on the main task. We look at targeted attacks, meaning that a training set of samples \hat{D} that represent the *target* inputs are classified as a specific target class t rather than their ground-truth class. For example, we might want to misclassify “all images containing a green car” as birds rather than vehicles, while not affecting the behavior for images of cars that are not green.

Attack Strategies The adversary can introduce a backdoor into the global model by submitting a malicious model update $\Delta\hat{\mathbf{w}}$ to the aggregation process. We consider two types of attack strategies to craft this malicious update. The first attack treats the training process as a blackbox and serves as a baseline. Here, the attacker’s capabilities are limited to

injecting malicious data points into its training dataset (i.e., data poisoning). The blackbox attacker crafts the malicious update by training on a poisoned dataset, using the same training algorithm \mathcal{A} as the benign clients, keeping the adversary’s model training hyperparameters (e.g. number of epochs and learning rate) the same as the benign clients’. For the second attack, the adversary is allowed to modify the local training process by applying a malicious training algorithm $\hat{\mathcal{A}}$. Here, the adversary crafts a malicious update using *model-replacement* [5, 74, 78], the state-of-the-art attack on FL systems. In model-replacement, the adversary *injects* the desired backdoor into their local model, and then applies scaling to amplify the update to survive aggregation.

Backdoor Injection. We assume that the attacker is in possession of both benign samples D_i and a set of backdoor samples \hat{D} , which represent the set of target inputs. The attacker crafts a malicious update by training on both sets of samples $D_i \cup \hat{D}$. Specifically, for every mini-batch of Stochastic Gradient Descent (SGD), the attacker ensures a balance between backdoor and benign samples, controlled by the poison ratio, i.e., the fraction of backdoor samples in each mini-batch.

Scaling. Scaling, also known as boosting [7], is used to amplify malicious updates to overpower benign updates [5, 7, 79]. In FL, updates are averaged using an aggregation function F , defined as $F(\mathbf{w}) = \sum_{i=0}^N \mathbf{w}_i \lambda_i$ with λ_i the relative weights of the clients. To ensure that its malicious update survives this aggregation, the attacker scales its update by a factor of γ (i.e., $\Delta\hat{\mathbf{w}}^{t+1} = \gamma(\hat{\mathbf{w}}^{t+1} - \mathbf{w}_G^t)$). This allows the attacker to exert outsized influence over the resulting global model. If the attacker can scale without any constraints, the attacker can essentially replace the global model completely by setting the scaling factor to $\gamma = \frac{\eta}{n}$, where η is the global learning rate and n the total number of clients. Under secure aggregation, the attacker can select γ freely without any constraints while the server remains unaware.

Bounded Scaling. Since scaling significantly increases the size of the malicious update, the aggregator can reduce the effectiveness of scaling attacks by enforcing an upper limit B on a p -norm of each client update such that $\|\Delta\hat{\mathbf{w}}\|_p \leq B$ [74, 78]. We assume that the attacker and clients are aware of this bound. Client i can ensure that their update fulfils this criteria via norm clipping, i.e., by scaling their update $\frac{\Delta\mathbf{w}_i}{\max(1, \frac{\|\Delta\mathbf{w}_i\|}{B})}$. The server rejects any update with a norm above the threshold. In this scenario, we consider an adversary that performs a state-of-the-art attack using Projected Gradient Descent (PGD) to adapt to the norm constraint [74, 78]. With PGD, the adversary constrains the solution space of $\Delta\hat{\mathbf{w}}$ so that the scaled update has a p -norm under the given bound (i.e., $\|\Delta\hat{\mathbf{w}}\|_p \leq \frac{B}{\gamma}$), to ensure the update complies with the norm bound.

2.2 Experimental Setup and Methodology

Tasks. In our analysis, we consider two tasks. Our first task (**FMN**) is a digit classification task on the Federated-MNIST dataset using a LeNet5 CNN architecture following [74, 78], with $n = 3383$ available clients and $m = 30$ clients selected per learning round. This dataset consists of samples from 3383 hand writers and is inherently non-IID because of the per-writer grouping, which simulates a natural distribution of training data. The second task (**C10**) is an image classification on the CIFAR-10 dataset using the ResNet18 [40] CNN with 273k parameters. We divide the dataset among $n = 100$ clients and select $m = 40$ clients in each round. We distribute the images to clients in a non-IID fashion using a Dirichlet distribution with parameter 0.9 in all dimensions. The hyperparameters we use throughout the experiments are provided in the appendix §A.1, and we make our analysis framework available online for the community to reproduce all experiments and facilitate further investigation of these attacks.

Study Approach. Initially, proposed targeted attacks [5, 7] in the FL setting necessarily relied on update scaling for success. However, more recently, it has been shown that attacks without active scaling can be successful if the attacker selects particular subsets of inputs as the attack target (i.e., edge-case samples) [78]. To understand why these attacks are possible, we analyze the types of attack targets in relation to insights on the nature of the input distribution of common deep learning tasks. Specifically, it has been widely observed that modern datasets of natural images and text data follow classical long-tailed distributions (e.g., the Zipf distribution) [33, 34, 76, 83]. The input distribution can therefore be modeled as a long-tailed mixture of *subpopulations*, i.e., a significant fraction of the samples in the dataset belong to rare subpopulations (e.g., images of cars from an unusual angle). We use this to categorize the inputs that are targeted by attacks, studying existing attacks with regard to two types of subpopulation that represent opposing ends of the input distribution. The first type are *prototypical* targets, i.e. subpopulations of samples that occur frequently in the dataset. The second type are *tail* targets, i.e. subpopulations that sit on the tail of the distribution. As a consequence, samples from these targets rarely occur in the benign clients’ datasets. We will show how similar attack strategies vary dramatically in effectiveness depending on the kind of subpopulation they target.

For the **FMN** task, we consider a backdoor attack targeting prototypical inputs that classifies images containing the number seven from 30 randomly selected hand-writers as the number one instead (**FMN-P**, 310 images in total), following [74]. For a tail backdoor attack, we follow [78] and use images of sevens from the ARDIS dataset that are mostly in the European style (with a horizontal bar in the middle), unlike the sevens in F-MNIST (**FMN-T**, 660 images). On the **C10** task, we use a prototypical backdoor attack from [5]: classifying images of green cars as birds (**C10-P**, 30 images). For the tail backdoor attack, we use images from airplanes of

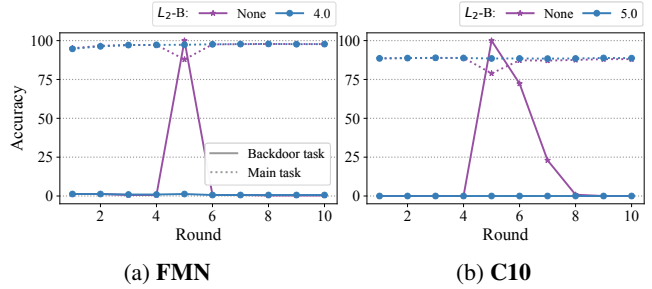


Figure 1: Single-Shot model-replacement attack [5] on a pre-trained model at round 5. The attacker can inject the backdoor in a single round by dominating the aggregation step using scaling.

Southwest airline that are collected by [78] to be introduced as tail backdoor images for CIFAR-10 (**C10-T**, 784 images). **Measuring Attacker Success.** For the **FMN-P** attack, attacker success is defined by the malicious classification accuracy on the backdoor images. For the **C10-P** attack, we measure accuracy using three backdoor samples that were not made available to the attacker during training. Test images are augmented into 200 versions per test image and used to evaluate the attacker success in the global model [5]. For the tail attacks (**FMN-T**, **C10-T**), the images are already grouped into train and test sets, the latter of which are used to evaluate accuracy.

Client Selection. For both tasks, a constant number of clients m is selected in every round. We assume that the attacker controls a fraction $\alpha \in [0, 1]$ of the selected clients and that the scaled malicious update is divided evenly over those clients.

2.3 Attacks on Prototypical Targets

We now examine attacks on prototypical subpopulations.

Single-shot Attack. Even an adversary controlling a single client (**FMN**: $\alpha = 3.3\%$, **C10**: $\alpha = 2.5\%$) that is selected in a single round can successfully inject a backdoor by scaling its update with a factor of 30 (**FMN**) and 100 (**C10**) respectively, as we can see in Fig. 1. The backdoor is injected in the fifth round, after the model already achieves high accuracy on the main task, i.e., updates from benign clients only marginally change the model. Though we discuss this attack in the context of prototypical subpopulations here, this attack is also effective on tail subpopulations. Server-side detection of such an attack is challenging, because the accuracy on the benign objectives does not significantly change and secure aggregation prevents the inspection client updates for abnormalities (i.e., scaling). To successfully inject the backdoor, the adversary relies on scaling to overpower the updates of other clients during aggregation. The ability of an attacker to introduce backdoors in this prototypical subpopulations setting is based on the adversary’s ability to scale its malicious contribution to overpower the benign clients’ contributions. Therefore, the question naturally arises whether we can pre-

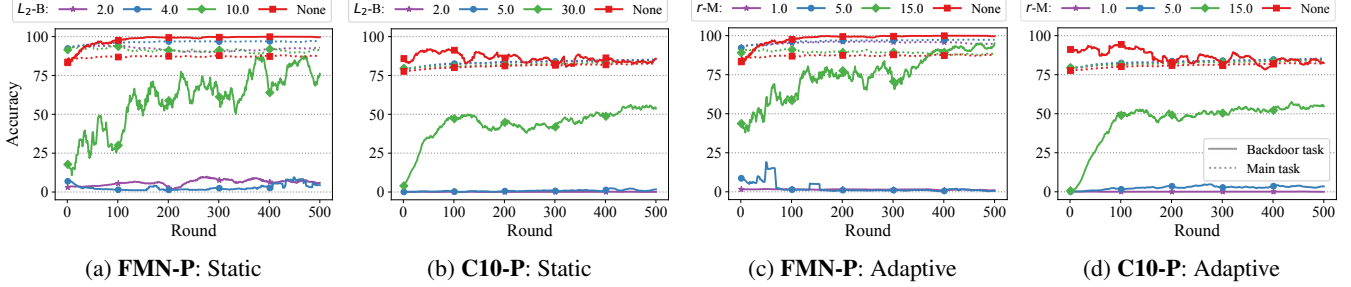


Figure 2: Continuous PGD attack under different static and adaptive norm bounds. The prototypical backdoor attack can be largely prevented by choosing an appropriate static or adaptive median-based norm bound.

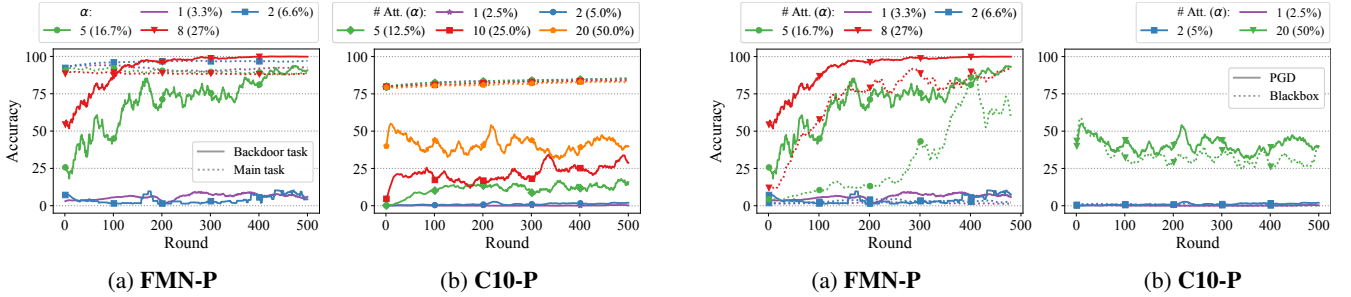


Figure 3: Continuous PGD attack for different fraction of compromised clients per round. As the number of attackers increase, the norm bound is decreasingly able to prevent the prototypical backdoor attack. (L_2 -norm bound, FMN: 2.0, C10: 3.0)

vent such attacks by restricting the clients’ ability to scale their contributions, for example, by enforcing bounds on the client inputs. Can we sufficiently limit the adversary’s ability to overpower the aggregation process? Indeed, an aggregator that enforces an L_2 -norm bound (FMN: 4.0, C10: 5.0) can prevent single-shot attacks, demonstrating the effectiveness of a constraint-based approach.

In the following, we investigate several aspects of the norm-bound defense to understand its potential, limitation, and practical deployment considerations. We start by evaluating the effectiveness of this defense in the presence of a continuous attacker, i.e., an adversary that controls a selected client in multiple rounds of FL training.

Continuous Attack. An attacker that is selected every round while controlling a single-client (FMN: $\alpha = 3.3\%$, C10: $\alpha = 2.5\%$) is inherently more powerful than a single-shot attacker and can inject a backdoor with the same strategy over many rounds (Fig. 2). The attacker can maintain a high accuracy (FMN: $> 95\%$, C10: $> 80\%$) on the malicious objective in the global model. As seen in Figs. 2a and 2b, limiting the scaling factor with an L_2 -norm bound, allows the aggregator to reduce the attacker’s success of injecting a prototypical backdoor. With a norm bound of 4.0 (FMN) and 5.0 (C10), the prototypical backdoor attack can be prevented with nearly no classification accuracy loss on the main task. Although the

Figure 4: Comparison of blackbox and PGD attack strategies for different fraction of compromised clients per round. The backdoor accuracy difference between the PGD and blackbox strategies is small. Main task accuracy is not shown for clarity, but can be found in Fig. 3. (L_2 -norm bound, FMN: 2.0, C10: 3.0)

attacker can send an update every round, the benign clients dominate the aggregation as the effect of scaling is limited by the bound. Note, that in this setting, we consider an attacker that uses PGD to adapt the model-replacement attacks to the norm constraints i.e., a more sophisticated version of the original scaling attack. We can also see from Figs. 2a and 2b that the choice of norm bound is important. If the server selects the bound too tight (i.e., 2.0 for FMN and C10), the convergence rate of the global model decreases as the honest clients have to clip their updates by a large margin. On the other hand, if the bound is too loose, the attacker can successfully inject the backdoor with larger scaling factors.

Adaptive Norm Bound. Choosing an appropriate norm bound is crucial for the effectiveness of the norm bound defense. However, selecting an effective norm bound is non-trivial. Many factors such as the model, data distribution, and even the progression of the training timeline can have an impact on the scope of benign model updates. For instance, benign client updates tend to get smaller as the model converges. Hence, the server could choose to modify the norm bound over time to be more effective. To adaptively determine a suitable norm bound, the aggregator can either estimate the bound using public datasets of the target classification task, or compute the bound from statistics over the updates that the

server can get by querying/probing the client. One method that we found to be practical for selecting the norm bound is to derive the bound from the median of the individual norms of client updates. This is a reasonable strategy as the median is robust against possible outliers from compromised clients for α below 50%. However, directly selecting the median as the bound can be too strict, slowing the convergence rate. To avoid this issue, the aggregator can introduce an additional parameter r by which the median is multiplied to determine the bound. In Figs. 2c and 2d, we show that choosing $r = 5$ will successfully prevent the attacks without impacting the convergence time of the main task.

Growing Number of Compromised Clients. So far, we considered an adversary that controls a single client in each round. In Fig. 3, we see that when the attacker controls more clients per round, the effectiveness of injecting a prototypical backdoor increases even if a norm bound is enforced. In these experiments, the strategy of the adversary is to divide the scaled malicious update among the compromised clients, i.e., the individual scaling factor for each malicious client becomes smaller. For **FMN**, we see that the malicious objectives’ success is below 10% for $\alpha \leq 6.6\%$, but above 80% for $\alpha \geq 16.7\%$. Similarly, for **C10**, the accuracy of the malicious objective is low for a small number of attackers ($\alpha \leq 6.6\%$), but gradually increases to 50% with $\alpha = 50\%$. We observe that if the attacker controls enough clients in each round, scaling becomes less relevant and the norm bound is less effective. This observation is supported by Fig. 4, where we can see a comparison of the model-replacement strategy with scaling against blackbox attacks that only alter the training data. The gap of attack success between non-scaled attacks (i.e., blackbox) and scaled attacks (i.e., model-replacement with PGD) decreases as the number of compromised clients increases. With $\alpha = 20\%$ compromised clients per round, the blackbox attack is already within 10% of the PGD attack accuracy. This suggests that, using norm bounding, we can eliminate or reduce the advantage an attacker gains from white-box training, to the point where the effectiveness of their attack is little better than that of honestly following the protocol and merely training over poisoned data. Of course, if an adversary can continuously influence a significant portion of the selected clients, the definition of FL implies that their (malicious) information will be incorporated into the global model. However, in real-world FL deployments, it is unlikely that an attacker will be able to continuously control a large portion of the clients each round, as they are selected randomly from a much larger pool of available clients.

2.4 Attacks on Tail Targets

So far, we discussed how attackers can embed backdoors in models by using scaling, which exploits the inherent susceptibility of the underlying linear aggregation rules used in FL. All the early targeted attacks for FL that were proposed [5, 7] relied on scaling for attack success. More recently, however,

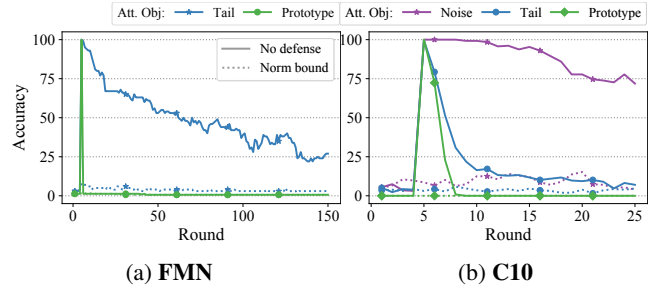


Figure 5: Comparison of prototypical and tail attack targets for the single-shot attack. Prototypical targets are quickly reversed by the honest clients, while tail targets stay in the model for a significantly longer time. (L_2 -norm bound, **FMN**: 4.0, **C10**: 5.0)

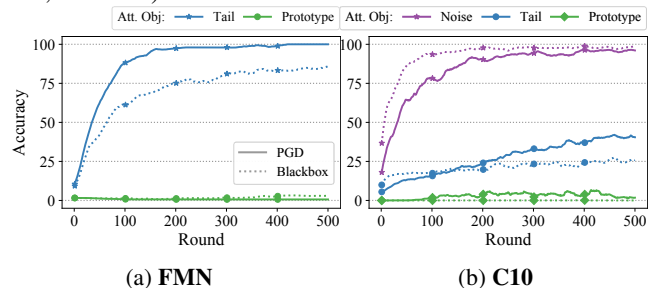


Figure 6: Comparison of prototypical and tail attack targets for the continuous attack under a norm bound. (**FMN**: $\alpha = 3.3\%$, L_2 -B: 1.0, **C10**: $\alpha = 12.5\%$, M - r : 1.5).

work has emerged that shows that introducing backdoors can be achieved without scaling if the attacker selects a particular subset of inputs as its attack target (i.e., tail samples) [78]. In the following, we provide insights on why this is possible and what aspect of the learning process these attacks exploit.

Single-shot Attack. Before we explore why these attacks are possible, we discuss some empirical observations comparing the performance of prototypical and tail attack targets for blackbox and PGD backdoor attacks. In Fig. 5, we can see a comparison between tail backdoors (**FMN-T**, **C10-T**) and prototypical backdoors (**FMN-P**, **C10-P**) for a single-shot attacker. We observe that a tail backdoor remains in the global model for a very long time (at least 200 rounds for **FMN**) after its initial introduction, while the prototypical backdoor is almost completely eliminated only a few rounds after its introduction. This is primarily because honest clients are unlikely to submit updates that strongly influence model behavior for the subpopulation of the tail backdoor since it is less likely that the benign clients’ training data contains data points from the tail of the distribution. However, when enforcing a norm constraint on the model updates, the tail single-shot attack also fails to inject the behavior successfully, as seen in Fig. 5. **Continuous Attack.** Next, we inspect how the attack target influences the adversarial success in the continuous setting. Fig. 6 shows that a tail backdoor can be injected without scaling if the attacker can participate over many rounds (100%

for **FMN** and 90% for **C10** after 500 rounds). In comparison, the prototypical backdoor attack’s success stays below 10% throughout the whole training process for both tasks. We can also observe that injecting the tail backdoor with high accuracy requires many FL learning rounds (i.e., over 500 rounds to achieve a good accuracy on the malicious objective). For tail targets, the attacker requires less influence in the aggregation process (i.e., scaling becomes less important) in order to be successful, as the malicious behavior is slowly learned by the global model. The advantage of a tail attacker using PGD over basic data poisoning (i.e., blackbox attack) is limited (15% accuracy advantage for both tasks), as can be seen in Fig. 6. The attacker can easily force the global model to memorize random samples, regardless of which attack strategy is used (see Fig. 6b). Both of these results indicate that these tail attacks inherently exploit the characteristics of the learning algorithm and not the aggregation rule itself.

Our results align with other empirical results [82] and a recent theoretical explanation [33, 34] that memorizing data at the tail of distribution is an inherent and essential property of modern over-parameterized learning models. ML Memorization in relation to data privacy has been explored in depth. Research shows that this is what enables membership inference attacks [72] or attacks that extract sensitive data from the model [19, 20]. However, with the emergence of learning paradigms such as FL that enable active attacks, memorization can also pose serious risks to robustness. Since it is memorization that allows attackers to embed tail backdoors, attackers need to only participate in the learning process with malformed data, otherwise following the protocol honestly. Even a single attacking client, participating over multiple rounds, is sufficient for the backdoor to be embedded persistently.

2.5 Discussion

As Machine Learning gets deployed in a wider range of settings, it has become clear that ML must move beyond simply pursuing accuracy and start to tackle important challenges in real-world deployments such as privacy and robustness. Federated Learning, though presenting many privacy benefits, amplifies ML robustness issues by exposing the learning to an active attacker that can be present throughout the training process and fine-tune their attacks to the current state of the model. In consequence, we have seen new and powerful attacks emerge that effectively impact FL integrity.

Attacks against secure FL can, with minimal effort (i.e., a single *scaled* malicious update in a single round) from the attacker, result in persistent backdoors in the model. However, as we have seen, norm bounding of client updates can effectively prevent or limit these attacks. Nevertheless, we show that there are situations where norm bounding is not sufficient. For example, an attack targeting the tail of the input distribution cannot be entirely prevented without sabotaging the ability of the model to learn less representative data point.

The requirement for machine learning algorithms to memo-

rize in order to learn tail subpopulations specific behavior [33] has largely been studied in the context of privacy. However, as we have shown in this analysis, it also has significant implication for ML integrity. Understanding this phenomenon in the context of ML robustness is of significant importance. Mechanisms that have been employed to limit memorization such as using appropriate regularization or noise addition are likely to also improve ML robustness for tail targets [33]. These countermeasures, however, introduce various tradeoffs with respect to accuracy, privacy, robustness, and fairness and are out of the scope of this paper.

In this analysis we show that norm bounding can provide meaningful practical robustness guarantees for FL. However, the privacy-preserving nature of secure-aggregation-based FL means that actually applying norm bounding is highly non-trivial. Relying on clients to self-regulate the sizes of their updates is obviously not viable in the presence of actively malicious attackers, and using standard secure computation tools would be highly impractical. Therefore, we need solutions that can enforce norm bounds over updates from untrusted clients, maintaining the privacy of client’s inputs. At the same time, the overhead must be small enough to enable practical deployments of FL in real-world settings.

3 RoFL Design

We start this section by presenting an overview of RoFL and then describe its cryptographic building blocks.

3.1 Overview

Setup. RoFL targets a standard FL deployment featuring a server coordinating a learning process with a large number of clients. In this deployment, the server periodically interacts with a subset of available clients to continuously improve its machine learning model. In each round of the training process, the server randomly selects m available clients and communicates the current global model to them. Each selected client i for $i \in \{1, 2, \dots, m\}$ then computes an ℓ -dimensional update vector $\mathbf{w}_i \in \mathbb{Z}_q^\ell$. Finally, the server uses secure aggregation to combine the clients’ updates in each round $\sum_{i=1}^m \mathbf{w}_i$ into a single update vector for the global model. The secure aggregation protocol ensures that the server does not learn anything about the clients’ updates \mathbf{w}_i beyond what can be learned from the final sum. The goal of RoFL is to allow the server to verify that the submitted client-updates \mathbf{w}_i are valid i.e., fulfill a pre-defined constraint while preserving the guarantees of secure aggregation and remaining compatible with the conventional deployment scenario. More specifically, RoFL allows constraining the L_p norm of client-updates \mathbf{w}_i i.e., $\|\mathbf{w}_i\|_p < B$ for some $B \ll q$, and we provide concrete instantiations for both L_∞ and L_2 norm bounds. Essentially, each selected client provides a proof that its update \mathbf{w}_i satisfies the bound. Upon receiving the client input, the server verifies that the proof is

valid. If the verification fails, the server discards the client input, and flags the client as corrupt.

Threat Model. We consider actively malicious clients but assume an honest-but-curious server, i.e., the server does not deviate from the protocol but analyzes received messages to try and gain information about clients’ private inputs. We also assume that the server can identify and authenticate clients. RoFL guarantees the confidentiality of client inputs. Specifically, neither the server nor an adversary that compromises a set of clients can learn anything beyond what they can derive from the the aggregation output. In addition, RoFL ensures that the server is able to detect if a client input \mathbf{w}_j does not fulfill a specified constraint defined by the server.

Our Approach. The FL setting poses unique compatibility and scalability challenges that render prior work on robustness in private aggregate statistics [24, 29, 44] inadequate or ineffective. The key challenge FL presents is that the client input to the aggregation consists of high-dimensional vectors that embody tens of thousands of values. Thus, the overall cryptographic costs can quickly become prohibitive in this setting.

To achieve high performance on realistic machine learning models, RoFL makes two key contributions. First, RoFL leverages an efficient and compatible zero-knowledge proof (ZKP) system to implement the targeted norm constraints under the existing secure aggregation protocol for FL [14]. The proof batching techniques of the underlying ZKP system reduce bandwidth requirements by several orders of magnitude. Second, RoFL proposes two optimizations to reduce the number of required cryptographic proofs to verify clients’ inputs which saves both bandwidth and computation.

In the following, we provide a high-level description of the cryptographic building blocks of RoFL (§3.2). Afterwards, we describe our protocol (§3.3) that uses these building blocks to enforce constraints on client inputs (§3.4). Finally, we introduce several optimizations that enable RoFL to scale to realistic machine learning models (§3.5).

3.2 Cryptographic Primitives

Commitments. A (*hiding*) *non-interactive commitment scheme* is an algorithm that allows an entity to commit to a value v while keeping it hidden, with the option to later reveal the committed value. Given a function $Com : M \times R \rightarrow C$, from a message space M and a randomness space R to a commitment space C , we compute a commitment to a value $v \in M$ as $c = Com(v, r)$ for $r \leftarrow R$. Opening a commitment, by revealing r and v allows the commitment to be verified by checking $c_v = Com(v, r)$. A commitment is *hiding* if it does not reveal any information about the committed value v . Furthermore, a commitment is *binding* if it is computationally infeasible to find v, r and v', r' such that $v \neq v'$ but $Com(v, r) = Com(v', r')$. **NIZK.** A *Zero-Knowledge Proof* (ZKP) is a statement that proves a fact to another entity without revealing additional information. For example, the prover might want to show that

they know the discrete log x of a group element g^x and that x lies in a specific range without revealing x . Traditionally, the prover would engage in an interactive challenge-response protocol with the verifier to prove a property about its private data. Using the Fiat–Shamir transform [35], these interactive ZKP protocols can be converted into a *Non-Interactive Zero-Knowledge Proof* (NIZK) [13]. The prover generates a single binary string π that can be used by any entity to verify the claim, without further interaction. For brevity, we refer to [17] for formal definitions of the security properties.

3.3 Secure Aggregation with Commitments

Commitments. For the client-updates \mathbf{w}_i we require a cryptographic primitive that: (*i*) provides confidentiality, (*ii*) is compatible with secure aggregation, i.e., is additively homomorphic, and (*iii*) supports efficient client-side zero-knowledge constraints. We identify commitments, more specifically Pedersen commitments [58], as an ideal building block for our design because they meet all requirements. In our protocol, a client i commits to each element of the vector \mathbf{w}_i and sends the resulting commitment vector \mathbf{c}_i to the server. In the following, we assume for simplicity that the vector \mathbf{w}_i is a scalar, denoted as w_i for client i . Note that this extends naturally to vectors with element-wise operations. Let \mathbb{G} be a cyclic group of prime order. To commit to an update $w_i \in \mathbb{Z}_q$, we select a generator g and a random group element $h \in \mathbb{G}$, choose a random value $s_i \in \mathbb{Z}_q$, and compute $c_i := g^{w_i} h^{s_i}$.

Pedersen commitments [58] are both hiding and binding under a standard discrete log hardness assumption. Furthermore, Pedersen commitments are additively homomorphic; thus allowing the server to aggregate parameters from each client without inspecting them. In addition, there exist efficient zero-knowledge range proofs [17] which are a natural fit to realize p-norm constraints and are directly compatible with this type of commitment.

Secure Aggregation. The server aggregates the commitments c_i using the additive homomorphic property of Pedersen commitments. Given two Pedersen commitments c_1 and c_2 for w_1 and w_2 , the product $c_1 \cdot c_2$ corresponds to a commitment for $w_1 + w_2$: $g^{w_1} h^{s_1} \cdot g^{w_2} h^{s_2} = g^{w_1+w_2} h^{s_1+s_2}$. The aggregated commitment is still hiding and therefore the server cannot learn the result. To enable the server to obtain the aggregated output, the m clients choose the nonces s_i in the commitments such that $\sum_{i=1}^m s_i = 0$. In essence, we are lifting the masking approach from [14] to the commitment-based setting. Therefore, the hiding factor cancels out when the aggregation is computed: $\prod_{i=1}^m c_i = g^{\sum_{i=1}^m w_i} h^{\sum_{i=1}^m s_i} = g^{\sum_{i=1}^m w_i}$. Finally, the server can derive the sum of all client-updates $\sum_{i=1}^m w_i$ by calculating the discrete logarithm to the base g . Note, while calculating the discrete logarithm of $y = g^x$ is hard for generic $x \in \mathbb{G}$, the aggregation result space in our domain is small (e.g., a 32 bit integer) and hence the discrete logarithm can be computed efficiently [59, 64].

Nonce Cancellation and Generation. The secure aggrega-

tion protocol requires that the random nonces cancel out for the server to recover the correct result. Since this cannot be verified from c_i alone. Therefore, we extend the Pedersen commitment to an ElGamal commitment by adding another group element committing to s_i . A well-formedness proof ensures that the same s_i is used. In the appendix (§A.6), we discuss this in more detail and also explain how we use a pseudorandom generator (PRG) to generate the nonces efficiently.

3.4 ZKP of Norm Bounds

Each client must provide a non-interactive zero-Knowledge (NIZK) proof that their committed update vector \mathbf{c}'_i is well formed and has a norm bounded by B where B is set by the server. RoFL offers two methods to select the norm bound adaptively for a training round, either the server uses public training data to compute an update and estimate a bound, or the median method presented in §2.3. Let \mathbf{w}_i be the parameter vector and \mathbf{s}_i the vector of canceling nonces of client i . In Camenisch and Stadler notation [18], a client needs to provide a proof of the following relation to the server:

$$\text{NIZK}(\mathbf{w}_i, \mathbf{s}_i) \{ \mathbf{c}'_i = (g^{w_i} h^{s_i}, g^{s_i}) \wedge \|\mathbf{w}_i\|_p < B \}$$

There exists a wide range of zero-knowledge proof systems (see Table 1 in [43]) to implement such proofs with different performance and security trade-offs. For FL workloads with a large number of parameters, we require a proof system that is as lightweight as possible on the client, has moderate bandwidth requirements (i.e., proof sizes), and has efficient realizations of range proofs compatible with homomorphic commitments required for norm constraints. RoFL uses Bulletproofs [17] because they provide linear time complexity for prover and verifier, they only have a logarithmic proof size, they do not rely on a trusted setup, they have a specialized efficient realization of range proofs with batching, and, lastly, they operate directly on Pedersen commitments.

We now introduce two variants of the protocol for norm constraints, starting with the more straightforward case of bounding the L_∞ norm where we can consider each parameter independently. We then show how to bound the L_2 norm, which depends on all parameters in the vector and which requires clients to additionally commit to, and prove range bounds over, the squares of each parameter. While this introduces significant additional costs in terms of communication and computation overheads, employing L_2 bounds is easier and more forgiving. Specifically, the lack of strict bounds on each parameter makes training less sensitive to tight bounds, while the overall bound still successfully prevents attacks.

L_∞ -Norm. To bound the L_∞ norm by B , it is sufficient for the prover to show to the verifier that each parameter w_j from \mathbf{w}_i is within a bounded range $w_j \in [0, B]$. For each committed parameter c_j , the client provides a zero-knowledge proof that $w_j \in [0, B]$ and that c_j was generated correctly. RoFL combines a standard non-interactive proof-of-knowledge of

discrete logarithm [18] for the correctness of the commitment, and the specialized efficient range-proof from Bulletproofs [17] for the range check. With Bulletproofs we can aggregate all ℓ (i.e., one for each parameter update) required range proofs into a single proof consisting of only $2(\log_2(b) + \log_2(\ell)) + 4$ group elements where b is the bit length of the range. In the context of FL, this reduces the bandwidth cost from linear in the number of parameters to a logarithmic (e.g., an improvement of 26000x for 100k parameters). Further, instead of mapping 32-bit floating-point parameters directly to \mathbb{Z}_q with standard fixed-point encoding, RoFL compresses parameters into b -bit integers using probabilistic quantization [42] (e.g. $b = 8$ or $b = 16$) without significant loss of accuracy in the overall model.

L_2 -Norm. Using the protocol from the L_∞ bound, we implicitly bound the L_2 norm by $\ell \cdot B^2$ but do not allow any parameter to exceed the bound B . To provide a more fine-grained bound for the L_2 norm, we append an additional proof to verify that the sum of squared parameters is bounded, i.e., $\sum_{i=1}^{\ell} w_i^2 < B_{L_2}^2$. For each committed parameter c_j , the prover provides an additional commitment to the square of the parameter, i.e. $c''_j = g^{w_j^2} h^{s''_j}$, and a proof that this is indeed a commitment to the square of the value committed to in c_j . This can be done with standard non-interactive proof-of-knowledge of discrete logarithm [18] by proving the knowledge of an opening to a Pedersen commitment by rewriting it to $c''_j = c_j^{w_j} h^{s''_j - w_j s_j}$. Additionally, the prover provides a proof that the sum of all c''_j 's in the vector lies in the range $[0, B_{L_2}^2]$. The verifier checks this by computing the same sum over all c''_j using the homomorphic property and checking the range-proof. Again, we use Bulletproofs [17] to instantiate the range proof. Note that since we are working in \mathbb{Z}_q , a malicious client might set some w_j to be very large so that the sum of squares overflows q . We therefore still require the individual range proofs over each w_j as in the L_∞ case. While we can bound them to any C so that $l \cdot C^2 < q$, in practice, it makes sense to choose C significantly smaller since proofs over smaller ranges are more efficient and individual parameters must be smaller than B_{L_2} so as not to push the L_2 -norm above $B_{L_2}^2$.

3.5 Optimizations

So far we have described the cryptographic building blocks of RoFL, and how our protocol via a careful co-build of cryptography and FL can achieve its performance. Despite these improvements, scaling the protocol to realistic neural network models remains challenging. Even as we optimize the cryptographic protocol to the specifics of FL, the sheer number of proofs required (i.e., number of model parameters) will result in a significant overhead. Thus, we explore how we can reduce the number of required proofs, by considering optimizations that take advantage of the particular combination of our protocol with the underlying FL model. First, we consider *probabilistic range checks* to optimize the L_∞ variant of our

protocol. Second, we present the application of a *compression* technique based on random subspace learning, compatible with our L_2 constraint. Finally, we discuss how we can utilize *optimistic continuation* to interleave the server-side verification of the previous round with client-side training for the next round. This significantly reduces the effective wall-time overhead introduced, at the cost of requiring a one-round rollback in case verification fails due to malicious activity.

Probabilistic Range-Checking (L_∞). For the L_∞ bound, the range proofs are by far the most significant component of the computation overhead (§4). In the base protocol, the client proves that each element in \mathbf{w}_i is smaller than the bound B . However, it turns out that it is not necessary to check all ℓ elements to detect a malicious client with high probability.

We can reduce the number of proofs by verifying only a random subset of the update vector. The key insight is that if the server selects the random subset *after* the clients have uploaded their commitments, the probability that at least one check fails for a malicious update can be modeled by a hypergeometric distribution. So we ask whether it is indeed necessary to prove that each element in \mathbf{w}_i is bounded to confirm that the client’s contribution is benign. In other words, can we reduce proofs by checking only a randomly selected subset of the parameters for the L_∞ variant of the protocol? We show that while this can introduce the possibility for an adversary to exceed the norm bound without detection, we can make this probability vanishingly small by separating the commitment step from the proving step in our protocol.

For example, assume a fraction $p_v \in (0, 1]$ of the ℓ parameters in an update exceed the bound and the server checks a fraction $p_c \in (0, 1]$ of the parameters. Selecting $p_c \cdot \ell$ elements below the bound when $p_v \cdot \ell$ are above follows a hypergeometric distribution. Thus, the probability of failing to detect the malicious behavior can be computed as $\text{Hyp}(p_c \cdot \ell | \ell, \ell \cdot (1 - p_v), p_c \cdot \ell)$. In Fig. 7, we show the number of parameters that we need to check to bound the failure probability by $\delta = 1e - 08$, for different assumptions about the fraction of parameters above the bound (p_v). In model replacement attacks with scaling, a significant portion of the weights exceed the bound (see §A.4), which makes probabilistic checking a desirable approach in practice. With this optimization, the clients send commitments and well-formedness proofs to the server but initially do not compute the range-proofs. After receiving all client updates, the server selects the random subset to be checked and communicates the selection to the clients. The clients then compute the range proofs only for this subset of parameters and send it to the server for verification. Note that since the commitments are binding, the clients are unable to change the already committed parameters. Unfortunately, this optimization cannot be applied in the L_2 norm variant, since even a single out-of-bound parameter in the update vector could lead to an overflow of the sum-of-squares proof. Essentially, this would allow an adversary to submit an arbitrary update vector while remaining undetected

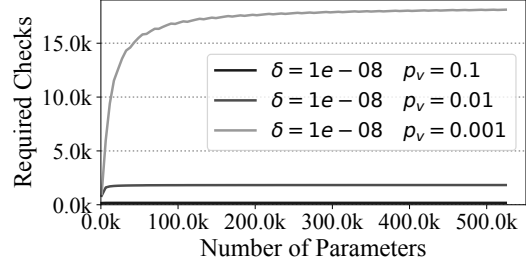


Figure 7: Number of update parameter ranges the server has to check with a failure probability of δ and the assumption that a fraction p_v of the parameters are above the bound.

with high probability.

Compression Techniques (L_2). Since both computation and communication overhead are linear in the size of the update vectors (§4), we can benefit from machine learning [42] compression techniques that reduce the size of the updates. However, the need to be compatible with secure aggregation and norm bounding limits the number of applicable techniques. In RoFL we experiment with random subspace learning [47] as an optimization, which was initially introduced in the context of understanding the hardness of machine learning tasks. Random subspace learning applies an L_2 -norm-preserving transformation that reduces the number of parameters required for a model update. Since the transformation preserves the L_2 -norm, the technique is compatible with our L_2 constraint. In random subspace learning, the model is trained in a random subspace W^d that has a lower dimension d than the original model’s dimension D . The random subspace W^d is projected onto the original model space W^D using an orthonormal projection matrix $P \in \mathbb{R}^{D \times d}$: $W^D = W_0^D + PW^d$. During training, W_0^D and P are treated as constants, and optimizations are done on W^d . Therefore, only W^d has to be exchanged between the client and server in each round, resulting in an improvement in the number of parameters from D to d . The parameter d , referred to as the *intrinsic dimension*, defines the compression ratio and has to be set by the server depending on the training task.

Optimistic Continuation. The computation time at the server is dominated by proof verification (§4). However, proof verification does not necessarily block the system from running the next training round, since the server already has access to the aggregation result (i.e., the global model of the next round). At the same time, the clients’ training usually takes significant time depending on the complexity of the model and the size of the client-dataset. In RoFL, we leverage this insight to execute the client training and the server proof verification in parallel. Upon receiving all client update vectors, the server optimistically aggregates the vectors and attempts to decrypt the sum, before distributing the resulting model to the clients participating in the next round. Should there be any inconsistencies e.g., a bound violation, the server aborts the new round and resets the model. However, since in-

consistencies should be infrequent in practice, this optimistic approach can reduce overall wall-time significantly as clients spend less time idling.

4 Evaluation

In this section, we answer the following questions, (i) what is the cost of integrating ZKP for norm bounds into secure FL protocols?, (ii) can our proposed optimizations improve scalability?, and (iii) is it possible to train a practical machine learning model with RoFL?

Implementation. We developed an end-to-end prototype of RoFL that we make available online. The framework enables training end-to-end machine learning models with secure aggregation in the FL setting and allow partitioners to specify constraints on the encrypted model updates. We implement the framework in Rust interfacing with Python to train neural networks with TensorFlow [30]. For client-server communication, we rely on the Tonic RPC framework [1] with protobuf. We use the elliptic curve Curve25519 (i.e., 126-bit security) implementation from the *dalek curve25519* library [28] for cryptographic operations. The library supports *avx2* and *avx512* hardware instructions for increased performance on supported platforms. The range proofs are implemented with the bulletproof library [27] that builds on the same elliptic curve library.

Microbenchmarks. We perform microbenchmarks to quantify the overhead of RoFL’s individual components using the Rust cargo benchmark module. For each reported result, we take the average of 4 measurements recorded after a single warm-up mock execution. We use a single AWS EC2 instance (c5d.4xlarge, 16 vCPU, 32GiB, Ubuntu18.04) with support for AVX512 instructions. To evaluate the performance of the microbenchmarks on more constrained client devices, we additionally perform the experiments on a less powerful AWS EC2 instance (t2.medium, 2 vCPU, 2GiB, Ubuntu18.04).

End-to-End benchmarks. We evaluate the end-to-end system performance on the same models as used in analysis: ResNet-18 [40] (CIFAR-10 L, 273k params) and LeNet5 (CIFAR-10 S, 62k params). In addition, we evaluate the performance for a model with a smaller amount of parameters (MNIST, 19k params). The MNIST model consists of two convolutional layers, a 2 by 2 max-pooling operation, and two fully connected layers. To simulate a practical deployment, we use five AWS EC2 instances (c5d.9xlarge, 36 vCPU, 72 GiB, Ubuntu18.04) with support for AVX512 instructions. The server uses one instance and the 48 clients are evenly distributed over the other four instances. In each training round, all 48 clients are selected.

4.1 Performance of Norm Bounding

We begin our evaluation by investigating the overhead of integrating ZKP proofs for the L_2 - or L_∞ -norm bound checks into secure aggregation on clients and the server. In the fol-

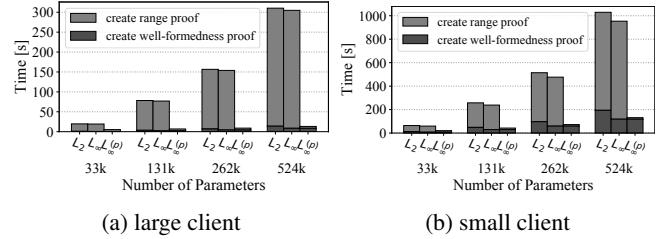


Figure 8: Client computation cost for committing to update vector and creating the L_2/L_∞ -norm bound proof.

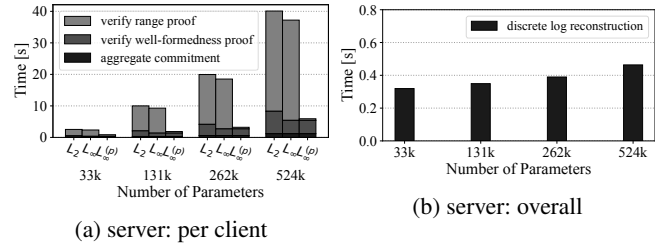


Figure 9: Server computation for zero knowledge proofs, commitment aggregation, and reconstruction of weight updates.

lowing, we first analyze the computation and bandwidth costs of the baseline protocol and then show the benefits of using our probabilistic checking optimization.

Computation. The client-side computational costs, beyond the federated learning protocol itself, only include the computation of commitments to each parameter and creating the corresponding zero-knowledge norm proofs. This additional cost is linear in the number of parameters, as seen in Fig. 8. On a strong client (Fig. 8a), the creation for L_2 and L_∞ proofs for 262k parameters takes 157 and 154 seconds, respectively, while on a less powerful machine (Fig. 8b), this cost increases by 3x to 514 and 477 seconds. These costs are predominantly determined by the actual range-proof creation, with the additional well-formedness proofs to ensure correct cancelling not contributing significantly. Note that while these costs are significant, they are within an order of magnitude of the model training cost, so clients that can efficiently perform the underlying FL computation should be able to handle the overhead, too. When using L_2 -norm proofs, clients need to compute additional proof-of-squares. However, this adds only a minor overhead compared to L_∞ -proofs. The server side, meanwhile, requires verifying the proofs of each client, aggregating them into the global vector, and reconstructing the aggregated vector once all updates are included. Similar to the client-side costs, the server-side verification and aggregate costs increase linearly with the number of parameters, as depicted in Fig. 9. With an update size of 262k (Fig. 9a), the server requires 19-20s per client to verify the norm proofs and aggregation where the verification of the range proofs dominates the processing time. Once the clients’ commitments are aggregated, the server has to solve the discrete log with the baby-step-giant-step algorithm for each parameter in

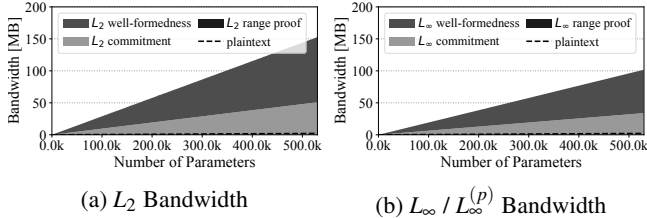


Figure 10: Additional bandwidth cost per client to upload the update to the server.

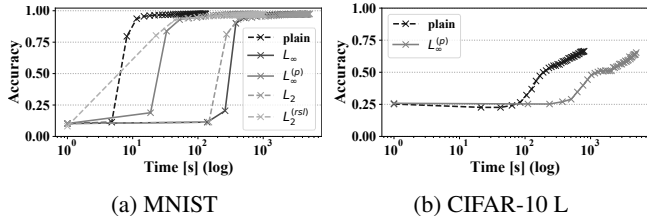


Figure 11: End-to-end convergence over time with different settings of RoFL.

the vector. Similar to the proof creation and verification, the discrete-log solving time increases linearly with the number of parameters, as shown in Fig. 9b. The server has to decrypt the aggregated vector only once per round independent of the amount of clients, which takes only 390ms for a vector of 262k parameters. Note that the tasks at the server are highly parallelizable and so we can reduce the overall computation time using horizontal scaling (i.e., adding more processors).

Bandwidth. In Fig. 10, we show bandwidth requirements for the commitments and proofs while varying the number elements in the update. The bandwidth requirements grow linear in the number of elements, but are higher for the L_2 -norm (Fig. 10a) compared to the L_∞ -norm (Fig. 10b), due to the additional commitments to the square and the corresponding proofs. The range proofs can be aggregated into a single proof, which has a size that increases logarithmically in the number of parameters in the update. Thus, the bandwidth costs are dominated by the commitment size and the additional group elements required for the well-formedness proof. For 262k parameters, the data transmitted to the server per client is 75MB (72x) for the L_2 -norm case and 51MB (48x) for the L_∞ -norm case, when compared to plaintext values with 32-bits per parameter. Clearly, this is a significant overhead that limits the size of model that this technique can scale to. Nevertheless, this is a significant improvement of four orders of magnitude over simply combining standard secure aggregation and sigma-protocol ZKP techniques. Finally, it is worth noting that while the *relative* size increase is dramatic, the absolute size of the updates is about the same as a few minutes of compressed HD video and therefore still well within the capabilities of most modern connections, including wireless and mobile connections.

Optimizations. We now show the improvements probabilis-

Type	Acc. [R40]	Computation Time			Bandwidth	
		Round [s]	Total [m]	Factor	Total [GB]	Factor
MNIST (19k params, rsl 5k params)						
plain	0.97	3	2	1x	0.3	1x
L_2	0.97	132	88	39x	10.8	37x
$L_2^{(rs)}$	0.97	26	17	8x	2.8	10x
L_∞	0.97	124	82	37x	7.2	25x
$L_\infty^{(p)}$	0.97	20	13	6x	7.2	25x
CIFAR-10 S (62k params, rsl 12k params)						
plain	0.54	2	1	1x	0.9	1x
L_2	0.54	282	183	134x	34.8	37x
$L_2^{(rs)}$	0.54	53	35	25x	6.7	7x
L_∞	0.54	252	164	120x	23.3	25x
$L_\infty^{(p)}$	0.54	38	25	18x	23.3	25x
CIFAR-10 L (273k params)						
plain	0.66	21	14	1x	4.2	1x
$L_\infty^{(p)}$	0.65	131	85	6x	102.8	25x

Table 1: Results of end-to-end model training for 40 rounds with RoFL.

tic checking of L_∞ has on the microbenchmarks evaluation of our protocol. We will defer discussion of the subspace learning optimization for L_2 to the end-to-end experiments, as this requires evaluating the trade-off between the number of parameters (i.e., compression) and the model accuracy. For this evaluation, we set a maximum failure probability of 10^{-8} and assume that at least $p_v = 0.005$ of the parameters in a malicious update exceed the bound (Fig. 7). Bandwidth-wise, probabilistic checking has only a negligible effect, since the aggregated range-proofs are already logarithmically sized (Fig. 10b). However, probabilistic checking can reduce the computation cost by 6x-17x for the clients and 6x for the server, as seen in Fig. 8 and Fig. 9a. Probabilistic checking really starts to shine when using larger numbers of parameters (e.g., from 154s to 9s on the large client, and 19s to 3s per client server-side for 262k params). Using probabilistic checking dramatically reduces the overhead of applying this protection while offering nearly the same level of protection. We believe that probabilistic checking is well suited to enhance the robustness of privacy-preserving FL in practical deployments.

Additional Setup Costs. The above experiments do not include the setup cost for establishing the canceling nonces with Diffie-Hellman key exchanges between the clients. Compared to the overheads of commitments and ZKPs these cost are small (i.e., 9KB bandwidth, and 24ms computation time per client and round for a 100 client setup).

4.2 RoFL End-to-End Performance

We demonstrate the effectiveness of RoFL in a practical deployment by showing that RoFL provides a significant speedup in terms of computation time compared to the unoptimized L_∞ - and L_2 -norm constraints. For the optimized version of the L_∞ -norm, we apply probabilistic checking while for L_2 , we compress the updates with subspace machine

learning to reduce the numbers of parameters. We evaluate RoFL for three models: MNIST (19k params), CIFAR-10 S (62k params), and CIFAR-10 L (273k params). We compare against an FL setup without any encryption or constraints using 32-bit plaintext values. For compatibility with the encryption used in RoFL, we apply 8-bit probabilistic quantization with 7 fractional bits to the floating point numbers of the client updates.

RoFL L_2 vs Plaintext. To optimize the L_2 -norm constraint in RoFL, we compress the updates using subspace machine learning to reduce the number of parameters. In the optimized experiments, the effective number of parameters (i.e., intrinsic dimension) of MNIST is 5000 (3.8x parameter reduction), and for CIFAR-10 S 12000 (5.2x parameter reduction) as explored in [47]. Table 1 compares the results of the different runs. In the MNIST task, our optimization enabled a reduction the training time per round from 64x to 13x compared to plaintext with the update compression. In the CIFAR-10 S experiment, we find that RoFL reduces the computation per round of 134x to 25x. We did not observe a noticeable impact on accuracy for the chosen intrinsic dimension for both models after 40 rounds. While further training might eventually make differences in final accuracy visible, our observations are in accordance with the reported accuracy in [47] for our selected intrinsic dimensions. In terms of bandwidth, the cost in this setting can be reduced with the compression from 37x to 10x for MNIST and from 37x to 7x for CIFAR-10 S, compared to the plaintext baseline.

RoFL L_∞ vs Plaintext. We show the use of probabilistic checking to optimize the L_∞ -norm constraint for different model sizes. In the optimized experiments, the server checks a number of parameters such that the probability that the adversary passes the check with more than 0.5% ($p_v = 0.005$) of parameters outside the bound is bounded by $1e-08$. Our optimization reduces the computation overhead in RoFL per round from 37x to 6x for MNIST, and from 120x to 18x for CIFAR-10 S. Despite the quantization to 8-bit fixed precision representation, the final classification accuracy on the model remains the same. While probabilistic checking is helpful even for smaller models, we start to see more significant speedups for larger models like the one used for the CIFAR-10 L task. Here, bandwidth costs do increase by 25x. However, end-to-end round times only increase from 21 seconds for a plaintext system to 131 seconds for our solution, an overhead of 6x. As a result, any system that can practically run the plaintext algorithm can likely also run our encrypted version in practice, albeit at a slightly reduced rate. Model convergence is similar for the plaintext and the secure settings, as shown in Fig. 11b, and accuracy is reduced by at most 1%.

5 Related Work

Addressing the challenges of robustness and privacy in machine learning is an active research area with a significant

body of work. In this section, we review related work in this space, focusing primarily on works that is relevant to RoFL.

Machine Learning Robustness. As machine learning models are increasingly deployed in sensitive settings, they are becoming a target for integrity attacks [11]. Consequently, attacks and defenses have been a topic of study by the security and machine learning communities. (i) *Attacks:* Modern machine learning pipelines are generally vulnerable to model evasion attacks at inference-time [8, 38, 75] and poisoning attacks at training-time [5, 7, 9, 10, 23, 41, 50]. Poisoning attacks either manipulate the input data [10, 23, 41, 50] or the model parameters directly [5, 6, 7, 32, 41], with the goal of reducing model performance (i.e., untargeted attacks) or integrating backdoors into the model (i.e., targeted attacks). The decentralized and distributed nature of FL exposes it to new attacks vectors [5, 7, 74, 78, 79] (ii) *Defenses:* Despite over a decade of research, machine learning robustness remains an open challenge. There have been several efforts that aim at defending against model evasion attacks [46, 53, 65] or mitigating poisoning attacks [26, 39, 49, 69, 73, 77]. These solutions assume that the server has access to the training data or has full control over the training process; both assumptions do not hold in FL, making these solutions non-applicable in this setting. In the collaborative setting, defenses have been proposed based on anomaly detection [36, 68] and Byzantine-robust estimators [12, 22, 57, 61, 80], but these assume direct access to client updates or training data. In addition, these defenses are greatly hampered by the large variance of client updates due to non-IID client data and high dimensionality of deep learning models in practical FL settings [6, 32]. Earlier work studying specific attacks [74, 78] indicates that clipping and noise addition can increase robustness, but did not further explore these solutions. In our analysis, we consider attacks more holistically and provide insights into when and why these techniques can be effective, laying the ground work for our design which realizes these constraints in an efficient and privacy-preserving way.

Secure Data Collection. Secure aggregation protocols [3, 21, 24, 44, 51, 52, 55, 60, 70] enable users to compute sums over their private data without disclosing the inputs. A variety of secure aggregation protocols have emerged to meet the needs of a wide range of applications introducing new security, scalability, and performance requirements. For brevity, we focus our review on secure aggregation systems most closely related to our work. Bonawitz et al. [14] introduce a secure aggregation protocol based on canceling random masks; their protocol builds on [3, 55] and is tailored to FL. Our protocol is similar to that proposed by Shi et al. [70]; however, ours is tailored to FL and does not assume a trusted setup. Both protocols do not enforce constraints on inputs in the face of malicious participants. Kursawe et al. [44] extend a variation of the protocol by Shi et al. [70] with ZKP to provide correct execution guarantees but does not constrain client inputs. A different body of work in this space [24, 25, 29]

considers a non-colluding trust model where the clients split the input values into shares and submit them to non-colluding servers. This enables efficient input checks, as expensive cryptographic operations can be avoided due to the assumption that the servers do not collude. However, we know from our discussions with FL industry players that organizations have struggled to deploy this trust model in practice, despite efforts to do so, e.g., using an external non-profit organization. Thus, the realistic deployment of the non-colluding trust model remains an issue hindering the deployment of these protocols in practice.

6 Conclusion

Federated Learning provides its privacy benefits by keeping the local training process, individual model updates, and data opaque to the server. However, in achieving this type of privacy, secure FL systems have to make sacrifices in terms of robustness. In this work, we show the inherent difficulties of achieving FL robustness via an empirical analysis that demystifies the inner working of existing attacks. To date, no compelling solutions exist that fully address robustness in secure FL. However, we show that constraints on client updates, such as norm bounds, can effectively limit a class of severe attacks. Toward this end, we develop RoFL, a system that augments the secure aggregation protocols in secure FL with efficient zero-knowledge proofs to enable input checks on the encrypted updates in practical settings. Despite this, a definite solution to FL robustness remains an open challenge and practitioners deploying FL need to proceed with caution. We hope that this work can help understand and distill the risks in open learning systems and will inspire follow-up works investigating FL robustness.

Acknowledgments

We thank Marko Mihajlovic, Matthias Lei, and Kenny Paterson for their valuable input and feedback. This work was supported in part by the SNSF Ambizione Grant No. 186050 and an ETH Grant.

References

- [1] Tonic RPC framework. Online: <https://github.com/hyperium/tonic>, May 2021.
- [2] Martin Abadi, Andy Chu, Ian Goodfellow, H Brendan McMahan, Ilya Mironov, Kunal Talwar, and Li Zhang. Deep learning with differential privacy. In *Proceedings of the 2016 ACM SIGSAC Conference on Computer and Communications Security*, pages 308–318, New York, New York, USA, 24 October 2016. ACM.
- [3] Gergely Ács and Claude Castelluccia. I have a DREAM! (Differentially private smart metering). In Tomáš Filler, Tomáš Pevný, Scott Craver, and Andrew Ker, editors, *Information Hiding*, volume 6958 of *Lecture Notes in Computer Science*, pages 118–132. Springer Berlin Heidelberg, Berlin, Heidelberg, 2011.
- [4] Alexander Viand, Patrick Jattke, Anwar Hithnawi. SoK: Fully Homomorphic Encryption Compilers. In *IEEE Symposium on Security and Privacy (SP)*, 2021.
- [5] Eugene Bagdasaryan, Andreas Veit, Yiqing Hua, Deborah Estrin, and Vitaly Shmatikov. How To Backdoor Federated Learning. In *AISTATS*, pages 2938–2948, 2020.
- [6] Gilad Baruch, Moran Baruch, and Yoav Goldberg. A Little Is Enough: Circumventing Defenses For Distributed Learning. In *NeurIPS*, volume 80, pages 8635–8645. 2019.
- [7] Arjun Nitin Bhagoji, Supriyo Chakraborty, Prateek Mittal, and Seraphin Calo. Analyzing federated learning through an adversarial lens. In *ICML*, pages 634–643, 2019.
- [8] Battista Biggio, Iginio Corona, Davide Maiorca, Blaine Nelson, Nedim Šrndić, Pavel Laskov, Giorgio Giacinto, and Fabio Roli. Evasion attacks against machine learning at test time. In *Joint European conference on machine learning and knowledge discovery in databases*, pages 387–402, 2013.
- [9] Battista Biggio, Blaine Nelson, and Pavel Laskov. Poisoning attacks against support vector machines. In *ICML, ICML’12*, pages 1467–1474, USA, 26 June 2012. Omnipress.
- [10] Battista Biggio, Blaine Nelson, and Pavel Laskov. Poisoning Attacks against Support Vector Machines. In *ICML*, page 1467–1474, 2012.
- [11] Battista Biggio and Fabio Roli. Wild Patterns: Ten Years After the Rise of Adversarial Machine Learning. In *ACM CCS*, 2018.
- [12] Peva Blanchard, El Mahdi El Mhamdi, Rachid Guerraoui, and Julien Stainer. Machine Learning with Adversaries: Byzantine Tolerant Gradient Descent. In *NeurIPS*, pages 119–129, 2017.
- [13] Manuel Blum, Paul Feldman, and Silvio Micali. Non-interactive zero-knowledge and its applications. In *ACM STOC*, pages 103–112. ACM, 1 January 1988.
- [14] Keith Bonawitz, Vladimir Ivanov, Ben Kreuter, Antonio Marcedone, H Brendan McMahan, Sarvar Patel, Daniel Ramage, Aaron Segal, and Karn Seth. Practical secure aggregation for Privacy-Preserving machine learning. In *ACM CCS*, pages 1175–1191, 2017.
- [15] Daniel Ramage, Brendan McMahan. Federated Learning: Collaborative Machine Learning.

- ing without Centralized Training Data. Online: <https://ai.googleblog.com/2017/04/federated-learning-collaborative.html>, 2017.
- [16] Theodora S Brisimi, Ruidi Chen, Theofanie Mela, Alex Olshevsky, Ioannis Ch Paschalidis, and Wei Shi. Federated learning of predictive models from federated electronic health records. *Int. J. Med. Inform.*, 112:59–67, April 2018.
- [17] Benedikt Bünz, Jonathan Bootle, Dan Boneh, Andrew Poelstra, Pieter Wuille, and Greg Maxwell. Bulletproofs: Short proofs for confidential transactions and more. In *IEEE Symposium on Security and Privacy (SP)*, pages 315–334, May 2018.
- [18] Jan Camenisch and Markus Stadler. Proof systems for general statements about discrete logarithms. *Technical report/Dept. of Computer Science, ETH Zürich*, 260, 1997.
- [19] Nicholas Carlini, Chang Liu, Úlfar Erlingsson, Jernej Kos, and Dawn Song. The Secret Sharer: Evaluating and Testing Unintended Memorization in Neural Networks. In *USENIX Security*, 2019.
- [20] Nicholas Carlini, Florian Tramer, Eric Wallace, Matthew Jagielski, Ariel Herbert-Voss, Katherine Lee, Adam Roberts, Tom Brown, Dawn Song, Úlfar Erlingsson, Alina Oprea, and Colin Raffel. Extracting training data from large language models. In *USENIX Security*, 2021.
- [21] Claude Castelluccia, Aldar C-F Chan, Einar Mykletun, and Gene Tsudik. Efficient and provably secure aggregation of encrypted data in wireless sensor networks. *ACM Trans. Sen. Netw.*, 5(3):20:1–20:36, June 2009.
- [22] Lingjiao Chen, Hongyi Wang, Zachary B. Charles, and Dimitris S. Papailiopoulos. DRACO: byzantine-resilient distributed training via redundant gradients. In *ICML*, pages 902–911, 2018.
- [23] Xinyun Chen, Chang Liu, Bo Li, Kimberly Lu, and Dawn Song. Targeted backdoor attacks on deep learning systems using data poisoning. *arXiv preprint arXiv:1712.05526*, 2017.
- [24] Henry Corrigan-Gibbs and Dan Boneh. Prio: private, robust, and scalable computation of aggregate statistics. In *USENIX NSDI*, pages 259–282, 2017.
- [25] Henry Nathaniel Corrigan-Gibbs. *Protecting Privacy by Splitting Trust*. PhD thesis, Stanford University, 2019.
- [26] Gabriela F Cretu, Angelos Stavrou, Michael E Locasto, Salvatore J Stolfo, and Angelos D Keromytis. Casting out demons: Sanitizing training data for anomaly sensors. In *IEEE Symposium on Security and Privacy (SP)*, pages 81–95, 2008.
- [27] Dalek Cryptography. Rust Bulletproofs Library. Online: <https://github.com/dalek-cryptography/bulletproofs>, August 2020.
- [28] Dalek Cryptography. Rust Curve25519 Library. Online: <https://github.com/dalek-cryptography/curve25519-dalek>, August 2020.
- [29] Yitao Duan, Netease Youdao, John F Canny, and Justin Z Zhan. P4P: Practical Large-Scale Privacy-Preserving distributed computation robust against malicious users. In *USENIX Security*, pages 207–222, 2010.
- [30] Martín Abadi et al. TensorFlow: Large-scale machine learning on heterogeneous systems, 2015. Software available from tensorflow.org.
- [31] Peter Kairouz et al. Advances and Open Problems in Federated Learning. *arXiv preprint arXiv:1912.04977*, 2019.
- [32] Minghong Fang, Xiaoyu Cao, Jinyuan Jia, and Neil Gong. Local model poisoning attacks to Byzantine-robust federated learning. In *USENIX Security*, pages 1605–1622, 2020.
- [33] Vitaly Feldman. Does learning require memorization? a short tale about a long tail. In *ACM STOC*, page 954–959, 2020.
- [34] Vitaly Feldman and Chiyuan Zhang. In *NeurIPS*, pages 2881–2891, 2020.
- [35] Amos Fiat and Adi Shamir. How to Prove Yourself: Practical Solutions to Identification and Signature Problems. In *CRYPTO*, pages 186–194, 1987.
- [36] Clement Fung, Chris J M Yoon, and Ivan Beschastnikh. Mitigating Sybils in Federated Learning Poisoning. *arXiv preprint arXiv:1808.04866*, 2018.
- [37] Ran Gilad-Bachrach, Nathan Dowlan, Kim Laine, Kristin Lauter, Michael Naehrig, and John Wernsing. CryptoNets: Applying neural networks to encrypted data with high throughput and accuracy. In *ICML*, pages 201–210, 2016.
- [38] Ian Goodfellow, Jonathon Shlens, and Christian Szegedy. Explaining and Harnessing Adversarial Examples. In *ICLR*, 2015.
- [39] Tianyu Gu, Brendan Dolan-Gavitt, and Siddharth Garg. Badnets: Identifying vulnerabilities in the machine learning model supply chain. *arXiv preprint arXiv:1708.06733*, 2017.
- [40] Kaiming He, Xiangyu Zhang, Shaoqing Ren, and Jian Sun. Deep Residual Learning for Image Recognition. *arXiv preprint arXiv:1512.03385*, 2015.
- [41] Yujie Ji, Xinyang Zhang, Shouling Ji, Xiapu Luo, and Ting Wang. Model-reuse attacks on deep learning systems. In *ACM CCS*, pages 349–363, 2018.

- [42] Jakub Konečný, H. Brendan McMahan, Felix X. Yu, Peter Richtarik, Ananda Theertha Suresh, and Dave Bacon. Federated Learning: Strategies for Improving Communication Efficiency. In *NeurIPS Workshop on Private Multi-Party Machine Learning*, 2016.
- [43] Ahmed Kosba, Dimitrios Papadopoulos, Charalampos Papamanthou, and Dawn Song. MIRAGE: Succinct Arguments for Randomized Algorithms with Applications to Universal zk-SNARKs. In *USENIX Security*, pages 2129–2146, 2020.
- [44] Klaus Kursawe, George Danezis, and Markulf Kohlweiss. Privacy-Friendly aggregation for the Smart-Grid. In *Privacy Enhancing Technologies*, pages 175–191. Springer Berlin Heidelberg, 2011.
- [45] Yann LeCun et al. LeNet-5, convolutional neural networks. <http://yann.lecun.com/exdb/lenet/>, 2015.
- [46] Mathias Lecuyer, Vaggelis Atlidakis, Roxana Geambasu, Daniel Hsu, and Suman Jana. Certified robustness to adversarial examples with differential privacy. In *IEEE Symposium on Security and Privacy (SP)*, pages 656–672, 2019.
- [47] Chunyuan Li, Heerad Farkhoor, Rosanne Liu, and Jason Yosinski. Measuring the Intrinsic Dimension of Objective Landscapes. In *ICLR*, 2018.
- [48] Mu Li, David G Andersen, Jun Woo Park, Alexander J Smola, Amr Ahmed, Vanja Josifovski, James Long, Eugene J Shekita, and Bor-Yiing Su. Scaling distributed machine learning with the parameter server. In *USENIX OSDI*, 2014.
- [49] Kang Liu, Brendan Dolan-Gavitt, and Siddharth Garg. Fine-pruning: Defending against backdooring attacks on deep neural networks. In *International Symposium on Research in Attacks, Intrusions, and Defenses*, pages 273–294, 2018.
- [50] Yingqi Liu, Shiqing Ma, Yousra Aafer, Wen-Chuan Lee, Juan Zhai, Weihang Wang, and Xiangyu Zhang. Trojaning Attack on Neural Networks. In *NDSS*, 2018.
- [51] Lukas Burkhalter and Anwar Hithnawi and Alexander Viand and Hossein Shafagh and Sylvia Ratnasamy. TimeCrypt: Encrypted Data Stream Processing at Scale with Cryptographic Access Control. In *USENIX NSDI*, 2020.
- [52] Lukas Burkhalter, Nicolas Kuchler, Alexander Viand, Hossein Shafagh, Anwar Hithnawi. Zeph: Cryptographic Enforcement of End-to-End Data Privacy. In *USENIX OSDI*, 2021.
- [53] Aleksander Madry, Aleksandar Makelov, Ludwig Schmidt, Dimitris Tsipras, and Adrian Vladu. Towards Deep Learning Models Resistant to Adversarial Attacks. In *ICLR*, 2018.
- [54] H Brendan McMahan, Eider Moore, Daniel Ramage, Seth Hampson, and Blaise Agüera y Arcas. Communication-Efficient learning of deep networks from decentralized data. In *AISTATS*, 2017.
- [55] Luca Melis, George Danezis, and Emiliano De Cristofaro. Efficient private statistics with succinct sketches. In *NDSS*, 2016.
- [56] Luca Melis, Congzheng Song, Emiliano De Cristofaro, and Vitaly Shmatikov. Exploiting unintended feature leakage in collaborative learning. In *IEEE Symposium on Security and Privacy (SP)*, pages 691–706, 2019.
- [57] Xudong Pan, Mi Zhang, Duocai Wu, Qifan Xiao, Shouling Ji, and Zheming Yang. Justinian’s GAAvernor: Robust Distributed Learning with Gradient Aggregation Agent. In *USENIX Security*, pages 1641–1658, 2020.
- [58] Torben Pryds Pedersen. Non-Interactive and Information-Theoretic secure verifiable secret sharing. In *CRYPTO*, pages 129–140. Springer Berlin Heidelberg, 1992.
- [59] J M Pollard. Monte carlo methods for index computation (mod p). *Mathematics of Computation*, 32(143):918, July 1978.
- [60] Raluca Ada Popa, Andrew J Blumberg, Hari Balakrishnan, and Frank H Li. Privacy and accountability for location-based aggregate statistics. In *ACM CCS*, pages 653–666, 2011.
- [61] Shashank Rajput, Hongyi Wang, Zachary Charles, and Dimitris Papailiopoulos. Detox: A redundancy-based framework for faster and more robust gradient aggregation. In *NeurIPS*, 2019.
- [62] Swaroop Ramaswamy, Rajiv Mathews, Kanishka Rao, and Françoise Beaufays. Federated Learning for Emoji Prediction in a Mobile Keyboard. *arXiv preprint arXiv:1906.04329*, 2019.
- [63] Nicola Rieke, Jonny Hancox, Wenqi Li, Fausto Milletari, Holger R Roth, Shadi Albarqouni, Spyridon Bakas, Mathieu N Galtier, Bennett A Landman, Klaus Maier-Hein, Sébastien Ourselin, Micah Sheller, Ronald M Summers, Andrew Trask, Daguang Xu, Maximilian Baust, and M Jorge Cardoso. The future of digital health with federated learning. *NPJ Digit Med*, 3:119, September 2020.
- [64] Hossein Shafagh, Anwar Hithnawi, Lukas Burkhalter, Pascal Fischli, and Simon Duquennoy. Secure sharing of partially homomorphic encrypted IoT data. In *ACM SenSys*, pages 29:1–29:14, 2017.
- [65] Ali Shafahi, Mahyar Najibi, Mohammad Amin Ghiasi, Zheng Xu, John Dickerson, Christoph Studer, Larry S

- Davis, Gavin Taylor, and Tom Goldstein. Adversarial training for free! In *NeurIPS*, pages 3358–3369, 2019.
- [66] Micah J Sheller, Brandon Edwards, G Anthony Reina, Jason Martin, Sarthak Pati, Aikaterini Kotrotsou, Mikhail Milchenko, Weilin Xu, Daniel Marcus, Rivka R Colen, and Spyridon Bakas. Federated learning in medicine: facilitating multi-institutional collaborations without sharing patient data. *Sci. Rep.*, 10(1):12598, July 2020.
- [67] Micah J Sheller, G Anthony Reina, Brandon Edwards, Jason Martin, and Spyridon Bakas. Multi-Institutional deep learning modeling without sharing patient data: A feasibility study on brain tumor segmentation. *Brainlesion*, 11383:92–104, January 2019.
- [68] Shiqi Shen, Shruti Tople, and Prateek Saxena. Auror: Defending against poisoning attacks in collaborative deep learning systems. In *ACM ACSAC*, pages 508–519, 2016.
- [69] Yanyao Shen and Sujay Sanghavi. Learning with bad training data via iterative trimmed loss minimization. In *ICML*, pages 5739–5748, 2019.
- [70] Elaine Shi, H T H Chan, Eleanor Rieffel, Richard Chow, and Dawn Song. Privacy-preserving aggregation of time-series data. In *NDSS*, 2011.
- [71] Reza Shokri and Vitaly Shmatikov. Privacy-Preserving deep learning. In *Proceedings of the 22nd ACM SIGSAC Conference on Computer and Communications Security, CCS ’15*, pages 1310–1321, New York, NY, USA, 2015. ACM.
- [72] Reza Shokri, Marco Stronati, Congzheng Song, and Vitaly Shmatikov. Membership inference attacks against machine learning models. In *IEEE Symposium on Security and Privacy (SP)*, pages 3–18, 2017.
- [73] Jacob Steinhardt, Pang Wei W Koh, and Percy S Liang. Certified defenses for data poisoning attacks. In *NeurIPS*, pages 3517–3529, 2017.
- [74] Ananda Theertha Suresh, Brendan McMahan, Peter Kairouz, and Ziteng Sun. Can you really backdoor federated learning? In *Federated learning workshop at NeurIPS*, 2019.
- [75] Christian Szegedy, Wojciech Zaremba, Ilya Sutskever, Joan Bruna, Dumitru Erhan, Ian Goodfellow, and Rob Fergus. Intriguing properties of neural networks. In *ICLR*, 2013.
- [76] Grant Van Horn and Pietro Perona. The Devil is in the Tails: Fine-grained Classification in the Wild. *arXiv preprint arXiv:1709.01450*, 2017.
- [77] Bolun Wang, Yuanshun Yao, Shawn Shan, Huiying Li, Bimal Viswanath, Haitao Zheng, and Ben Y Zhao. Neural cleanse: Identifying and mitigating backdoor attacks in neural networks. In *IEEE Symposium on Security and Privacy (SP)*, pages 707–723, 2019.
- [78] Hongyi Wang, Kartik Sreenivasan, Shashank Rajput, Harit Vishwakarma, Saurabh Agarwal, Jy-yong Sohn, Kangwook Lee, and Dimitris Papailiopoulos. Attack of the Tails: Yes, You Really Can Backdoor Federated Learning. In *NeuroNIPS*, pages 16070–16084, 2020.
- [79] Chulin Xie, Keli Huang, Pin-Yu Chen, and Bo Li. DBA: Distributed Backdoor Attacks against Federated Learning. In *ICLR*, 2020.
- [80] Dong Yin, Yudong Chen, Ramchandran Kannan, and Peter Bartlett. Byzantine-Robust Distributed Learning: Towards Optimal Statistical Rates. In *ICML*, 2019.
- [81] Chengliang Zhang, Suyi Li, Xia Junzhe, , Wei Wang, Feng Yan, and Liu Yang. BatchCrypt: Efficient Homomorphic Encryption for Cross-Silo Federated Learning. In *USENIX ATC*, 2020.
- [82] Chiyuan Zhang, Samy Bengio, Moritz Hardt, Benjamin Recht, and Oriol Vinyals. Understanding deep learning requires rethinking generalization. In *ICLR*, 2017.
- [83] Xiangxin Zhu, Dragomir Anguelov, and Deva Ramanan. Capturing long-tail distributions of object subcategories. In *IEEE CVPR*, pages 915–922, 2014.

A Appendix

A.1 Experimental Setup

We present the details of the experiments in analysis and evaluation. We would like to note that all code including a full specification of each experiment in configuration files is available online⁴.

Analysis We consider two image classification tasks that have been used before in the context of FL backdoor attacks to provide comparison to previous work. The first task (**FMN**) is a digit classification task on the Federated-MNIST dataset. The Federated-MNIST dataset consists of samples from 3383 hand writers. Since the samples are grouped by hand writer, the dataset simulates a natural distribution of training data. The second task (**C10**) is an image classification on the CIFAR-10 dataset, where the samples are distributed in a non-IID fashion using a Dirichlet distribution with parameter 0.9 in all dimensions. The full hyperparameters for the setups of **FMN** and **C10** are shown in Table 2. For **C10**, we use data augmentations (random horizontal flips and shifts) to increase the size of the dataset.

The global learning rate η controls the fraction of the model that is updated each round. For **FMN**, the full model is updated with the average of $m = 30$ client updates ($\eta = \frac{3383}{30}$).

⁴<https://github.com/ppps-lab/rofl-project-code>

Client	FMN	C10
# Training samples	341873	50000
Model	LeNet5	ResNet-18
# Classes	10	10
# Total number of clients	3383	100
# Selected clients per round	30	40
# Local training epochs per round	5	2
Batch size	32	64
Optimizer	SGD	
Learning rate	0.01	0.02

Table 2: Hyperparameters for honest clients.

For **C10**, we follow [5] and use a global learning rate of 1, indicating that 40% of the model is replaced every round. We pre-train the models for both tasks once and use the same weights as a starting point for each experiment, similar to [78]. The pre-trained models have not yet fully converged, to show the effect of different configurations on model convergence. For **FMN**, we use a pre-trained LeNet5 with 88% test accuracy and for **C10** we use a ResNet-18 with 80% test accuracy. The full configuration of the models are given in §A.3. All experiments in analysis except those in Figs. 1 and 5 show the accuracy as a moving average with a window size of 20, to improve readability.

Evaluation The configuration of the end-to-end setup experiments are similar to those of the analysis, except for some minor changes. For instance, we increase the number of clients in the evaluation to 48 to benchmark the performance of a larger deployment. For MNIST, we use a learning rate of 0.1, for CIFAR-10 S a learning rate of 0.075 and for CIFAR-10 L a learning rate of 0.01.

A.2 Attack configuration

We discuss the configuration of the backdoor injection attacks used by the adversary to create a malicious model update. We explore two attack strategies: the blackbox strategy and the model-replacement strategy [5]. In the blackbox strategy, the attacker follows the training process (i.e., hyperparameters) as the benign clients, but is allowed to insert a number of malicious samples into each batch according to the poison ratio. For the model-replacement strategy, the attacker first performs malicious training to create a malicious update, and then scales this update to overpower the other clients in the aggregation process.

In both strategies, the compromised clients train the model for a fixed amount of SGD steps, determined by the number of epochs and batches shown in Table 3. Each batch contains benign samples, and a number of target samples mislabeled with the target class. The amount of malicious samples in each batch is controlled by the poison ratio. The optimal

Setup	FMN	C10
# Local training epochs per round	10	6
# Batches	25	10
Batch size	32	64
# Poison samples per batch	12	20
Optimizer	SGD	
Learning rate	0.1	0.1
Scale factor	30	100

Table 3: Hyperparameters for model replacement attack

backdoor injection attack also includes benign samples because it allows the attacker to move the model into a direction where both objectives are satisfied simultaneously, making the attacker’s update harder to reverse by honest client updates [5, 78]. We apply learning rate decay to malicious training to ensure the model update has a good accuracy on both the main and backdoor tasks. The learning rate starts at 0.1 and decays step-wise with $\frac{1}{10}$ every $\frac{1}{3}$ of the total number of steps. When an L_p -norm bound B is present, the adversary uses Projected Gradient Descent (PGD) to adaptively craft malicious updates. Concretely, after every SGD step, we project the model update $\Delta\hat{\mathbf{w}}$ back to the closest point inside the space permitted by the norm bound such that $\|\Delta\hat{\mathbf{w}}\|_p \leq \frac{B}{\gamma}$, where γ is the scaling factor. More precisely, similar to [78], during an epoch we project the update back onto a slightly larger space $1.2\frac{B}{\gamma}$. Only, after the last SGD step of the epoch, we use γ as a scaling factor to satisfy the norm constraint (Table 3). In practice, this approach leads to a higher attacker success, similar as to what was reported in [78].

A.3 Model architectures

We describe the model architectures used both in the analysis and in the evaluation (end-to-end) experiments.

LeNet5 We make use of the standard LeNet5 [45] convolutional neural network for both **FMN** in the analysis and CIFAR-10 S. Note that the input layers for both applications of the model are different: 28-by-28, 1 channel for **FMN** and 32-by-32, 3 channels for CIFAR-10 S.

ResNet18 We use the ResNet [40] model for experiments in the analysis (**FMN**) as well as in evaluation experiments (CIFAR-10 L). We use the ResNet implementation provided by the Keras ResNet CIFAR-10 example⁵, corresponding to the ResNet20v1 model.

CNN For the small MNIST model used in evaluation, we use a standard convolutional neural network (CNN) architecture, consisting of two convolution layers of 8 and 4 filters, respectively, with kernel size 3-by-3. These are followed by a 2-by-2

⁵https://github.com/rstudio/keras/blob/master/vignettes/examples/cifar10_resnet.py

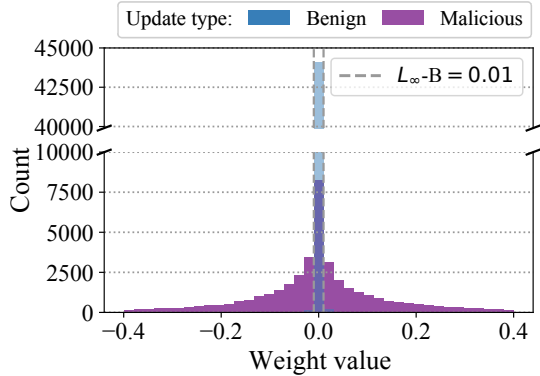


Figure 12: Weight distribution of a malicious update (FMN, FMN-P). Parameters outside of the interval $[-0.4, 0.4]$ are not shown (5004 weights for the malicious update, 0 for the benign update).]

max-pooling layer, a fully connected layer of 32 units and then the output layer. The model has 19k trainable parameters.

A.4 Probabilistic Checking

To optimize the L_∞ -norm bound we use probabilistic checking to reduce the amount of zero-knowledge proofs that must be created and verified. This optimization relies on the idea that the attacker has to send many parameters outside the bound to dominate the aggregation through scaling, while the server only has to find a single parameter violating the bound to identify a malicious update. The probability of detection follows a hypergeometric distribution, which increases quickly with the number of checked parameters.

We show the weight distribution of a benign and a malicious update in Fig. 12. We can see that a significant portion of weights of the malicious update lie outside the L_∞ -norm bound of 0.01 (Fig. 14). This is a suitable norm bound for this setup, For the malicious update, 36320 parameters (81.8%) lie outside the bound, versus only 385 parameters (0.87%) for the benign update. We show the progression of the number of parameters that are outside the bound over multiple rounds in Fig. 13. At the beginning of the attack in round 1, the malicious update has at least 81.8% of parameters above the bound of 0.01. This percentage decreases over time to around 47.1% on average in round 500, as the backdoor already exists in the model in later rounds. We can see that this percentage is well above the $p_v = 0.005$ (0.5%) assumed in the evaluation.

A.5 Additional experiments

We present additional experiments for the robustness analysis in this section.

L_∞ -norm We demonstrate in Fig. 14 that an L_∞ -norm bound can protect against prototypical backdoor attacks, similar to

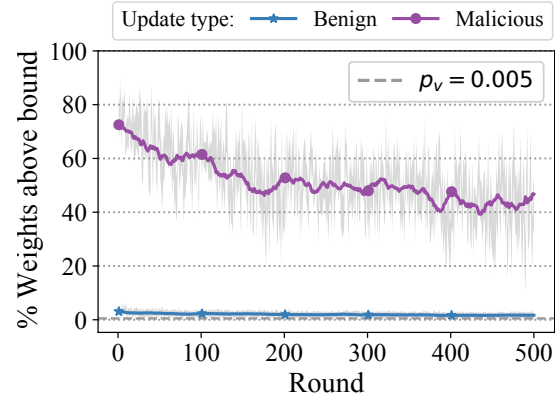


Figure 13: Percentage of weights outside the L_∞ -norm bound of 0.01 for malicious and benign clients per round (FMN, FMN-P). The total number of weights is 44426. We plot the assumption $p_v = 0.005$ as used in the evaluation.

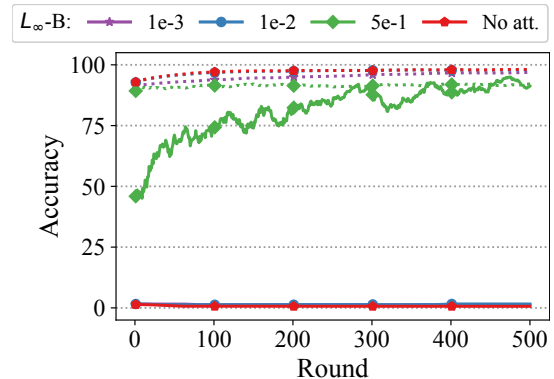


Figure 14: Comparison of PGD attack under different static L_∞ -norm bounds (FMN).

an L_2 -norm bound. An L_∞ -norm bound of 0.01 is sufficient to successfully defend against a backdoor attack on prototypical samples, without impacting model convergence or accuracy. Similar to the L_2 -norm bound, when the norm bound is too tight, model convergence is impacted. Conversely, when the bound is too loose, the attacker is able to successfully inject the prototypical backdoor into the model.

Additional comparison of attack targets In Fig. 15, we show the performance of a continuous attack for prototypical and tail targets under a median-based norm bound. This is the same experiment as in Fig. 6a, but for an adaptive norm bound instead of a static norm bound.

A.6 Nonce Cancellation and Generation

Ensuring Nonce Cancellation. The secure aggregation protocol requires that the random nonces cancel out for the server to recover the correct result. However, the server cannot verify that this is the case from the c_i alone. To overcome this

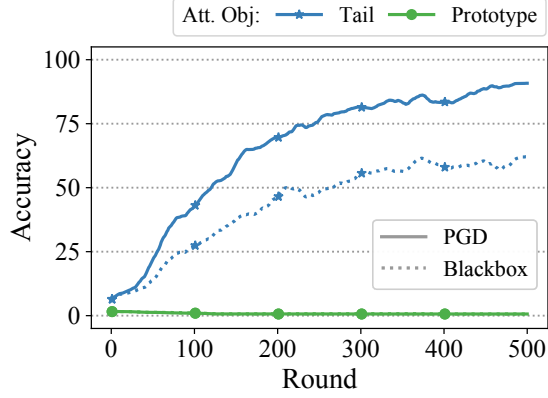


Figure 15: Comparison of prototypical and tail attack targets for the continuous attack under a norm bound. (FMN: $\alpha = 3.3\%$, M-r: 1.0).

problem, we extend the Pedersen commitment to an ElGamal commitment, by adding a group element committing to s_i :

$c'_i = (c_i, \tilde{c}_i) = (g^{w_i} h^{s_i}, g^{s_i})$. A well-formedness proof ensures that the same s_i is used (§3.4). ElGamal commitments are also binding, hiding, and additively homomorphic. The addition of g^{s_i} allows the server to check if the randomness cancels out since $\prod_{i=1}^m \tilde{c}_i = 1 \Leftrightarrow \sum_{i=1}^m s_i = 0$.

Nonce Generation. For the nonce generation, we follow the original protocol [14], deriving the nonce s_i of each client from pairwise shared secrets between the clients. For each pair (i, j) of clients with $i < j$, the two clients agree on a shared random secret $k_{i,j}$. Client i adds $k_{i,j}$ to its nonce s_i while client j subtracts $k_{i,j}$ from its nonce s_j . In total, the nonce of client i is therefore: $s_i = \sum_{i < j} k_{i,j} - \sum_{i > j} k_{j,i} \pmod q$.

Note that, while the sum of all nonces cancels out to zero, any partial aggregation includes at least one non-cancelled nonce and thus remains indistinguishable from random. When sending an entire update vector of dimension ℓ , clients use $k_{i,j}$ as the seed value for a pseudorandom generator (PRG) to generate many shared secrets.